

Inherent Structures of Crystalline Tetracene

Raffaele Guido Della Valle,* Elisabetta Venuti, and Aldo Brillante

Dipartimento di Chimica Fisica e Inorganica and INSTM-UdR Bologna, Università di Bologna, Viale Risorgimento 4, I-40136 Bologna, Italy

Alberto Girlando

Dipartimento di Chimica G.I.A.F. and INSTM-UdR Parma, Università di Parma, Parco Area delle Scienze, I-43100 Parma, Italy

Received: February 21, 2006; In Final Form: June 20, 2006

We have systematically sampled the potential energy surface of crystalline tetracene to identify its local minima. These minima represent all possible stable configurations and constitute the “inherent structures” of the system. The crystal is described in terms of rigid molecules with Coulombic and atom–atom interactions. Hundreds of distinct minima are identified, mostly belonging to the space groups $P\bar{1}$ (triclinic) and $P2_1/c$ (monoclinic), with a variety of structural arrangements. The deepest minimum corresponds to the high temperature–low pressure polymorph. This is the only polymorph with a completely described X-ray structure, which is satisfactorily described by the calculations. The next deep minimum is likely to correspond to the low temperature–high pressure polymorph, which has been experimentally identified but not yet fully described.

1. Introduction

Tetracene and pentacene show the highest charge mobilities among organic semiconductors and are thus recognized as promising materials for applications in electronic and optoelectronic devices.^{1–3} For these compounds it has been found that several polymorphs exist^{4–11} and that control of the crystallization conditions is crucial for the achievement of optimal performances in charge carrier mobilities.^{12,13}

In a past research project,^{14–19} we combined computational and experimental methods to investigate the polymorphs of crystalline pentacene. Initially, on the computational side, we identified the crystallographic structures at the local minima of the potential energy. These minima correspond to the possible configurations of mechanical equilibrium and thus constitute the “natural” or “inherent” structures that the system can exhibit.²⁰ Either by starting from all available X-ray structures^{14,15} or by systematically sampling the configuration space,¹⁶ we predicted a number of possible polymorphs. The X-ray structures^{6–9} converge either to the first^{6–8} or to the second⁹ deepest minimum and thus correspond to the two most stable polymorphs. Further deep minima with layered structures were also predicted. These might correspond to the thin film polymorphs found to grow on substrates^{4,5} and not yet fully described. On the experimental side, we could readily confirm the existence of two distinct polymorphs by identifying two different crystal morphologies, characterized by clearly different Raman spectra in the region of the lattice phonons.^{16,17} The identity of the samples, initially assigned only by matching experimental and calculated spectra, was finally verified directly with X-ray diffraction measurements.¹⁹

Encouraged by the success with pentacene, we have applied an analogous combination of experimental and computational methods to tetracene. Complete X-ray measurements are available for a first triclinic polymorph with space group $P\bar{1}$ (C_1^1), identified first at room temperature^{9,10} and then at 183 K.⁸ The unit cell contains two inequivalent molecules ($Z = 2$) located

on inversion sites. A second triclinic polymorph¹¹ has been identified by X-ray diffraction at 140 K. Unit cell parameters, but no atomic coordinates, have been obtained. The space group, which has not been determined,¹¹ may be either $P1$ or $P\bar{1}$. To tackle the problem of tetracene, we initially analyzed the Raman spectra of the lattice phonons as a function of pressure and temperature,²¹ identifying two distinct polymorphs characterized by clearly different spectra, polymorph I and II. Either polymorph can be observed at room conditions, depending on the method of preparation and on the history of the samples. Polymorph I is the most frequently grown form, stable at room conditions.²¹ Polymorph II is the form obtained either by lowering the temperature below 140 K or by increasing the pressure well above 1 GPa.^{11,21–23} However, it can be obtained²¹ also as a (probably metastable) phase at room conditions. For both polymorphs, the Raman spectra are consistent with $P\bar{1}$ structures with $Z = 2$, while a $P1$ structure appears extremely unlikely.²¹

Our calculations confirm that all the complete X-ray structures, obtained either at room T ^{9,10} or at 183 K,⁸ really belong to a unique polymorph (polymorph I),²¹ since the same potential energy minimum is reached by starting from each one of them. We have now sampled the potential energy surface²¹ to obtain information on the possible occurrence of different structures and on the relative stability of the various minima. We show that polymorph I^{8–10} certainly corresponds to the deepest minimum. Polymorph II,¹¹ identified at 140 K, most likely corresponds to the next deepest minimum, but this cannot be established unambiguously.

In the present paper we discuss the sampling strategy and provide theoretical information on the overall distribution of minima, while searching for the possible emergence of trends and regularities. We find many similarities with the case of pentacene, together with some significant differences. For tetracene, in fact, we notice a reduced variety of structures and a much larger energy spread for the deepest minima. This

behavior, which indicates a less rugged potential surface, may be connected to the observation that tetracene polymorphs are not as readily formed as those of pentacene.

2. Calculations

Since most computational methods are identical to those extensively discussed in the work for pentacene,¹⁶ only a brief description is presented here. A quasi-random sampling method, known as a low-discrepancy Sobol' sequence,²⁴ was used to generate 2500 different initial triclinic structures with two independent molecules for the unit cell. The molecules were treated as rigid units with the ab initio geometry computed using a 6-31G(d) basis set in combination with an exchange-correlation functional B3LYP.²⁵ The intermolecular potential was represented by an atom-atom Buckingham model²⁶ with Williams parameter set IV,²⁷ combined with a Coulombic contribution described by a set of atomic charges fitted to the electrostatic potential (ESP charges).²⁸ Starting from each initial structure, we performed steepest descent energy minimizations of the total potential Φ , by adjusting cell axes, cell angles, positions, and orientations of the molecules. About 30% of the configurations failed to converge to compact and stable bound states with positive vibrational frequencies of the lattice and had to be discarded. The structures at the potential minima were finally analyzed to discover their space group and to identify all minima encountered more than once. Cell doubling or halving was occasionally necessary at this stage to escape from saddle points with nonpositive frequencies or to obtain a conventional crystallographic cell.^{29,30} The efficiency of the search process was analyzed by monitoring the number of distinct minima. Since by increasing the coverage of the search space we approach a saturation plateau where new configurations tend to fall more and more frequently onto previously encountered minima, we have probably identified a large part of the accessible minima. Further searching appears unnecessary.

The calculations were mostly performed with available computer programs, which include GAUSSIAN98²⁸ for the ab initio geometry and charges, WMIN³¹ for the potential energy minimization, IONIC³² for the lattice frequencies, PLATON³³ for the identification of the space groups, and MOLSCRIPT³⁴ for the molecular graphics. As discussed for pentacene,¹⁶ additional codes also had to be developed.

3. Results

3.1. Classification of the Minima. Once we completed the search, we were left with 268 *distinct* minima in eight different space groups, with triclinic, monoclinic, and orthorhombic lattices. Following the procedure used for pentacene,¹⁶ we classify these minima according to their structural class,^{35,36} which completely characterizes the number and type of independent structural parameters. This analysis, presented in Table 1, yields 13 different structural classes, with up to four independent molecules in the unit cell. The distribution of minima among the various space groups and structural classes is similar to that found for pentacene.¹⁶ Like for pentacene, the two most frequent space groups are $P\bar{1}$ and $P2_1/c$, which are also the most frequent groups found in the statistical surveys on the experimental structures of molecular crystals.³⁵⁻³⁷ These two groups together account for $\approx 97\%$ of the distinct minima, while for pentacene they covered $\approx 89\%$ of the distinct minima.¹⁶ As typical examples of the structures we have chosen a subset of the minima, which includes the lowest minimum in each structural class and a few other deep minima. Drawings of all selected structures appear in Figure 1. For each of these

TABLE 1: Minima Classified by Structural Class^a

lattice type	space group	Z	site symmetry	N of minima	
				distinct	total
triclinic	$P1 (C_1^1)$	2	(1, 1)	5	6
	$P\bar{1} (C_i^1)$	2	($\bar{1}$)	3	3
		1	($\bar{1}$)	22	385
		2	($\bar{1}, \bar{1}$)	168	902
		4	($\bar{1}, \bar{1}, \bar{1}$)	6	14
monoclinic	$P2_1 (C_2^2)$	2	(1)	2	2
	$C2 (C_2^3)$	4	(1)	1	1
	$P2/c (C_{2h}^4)$	2	(1)	1	1
	$P2_1/c (C_{2h}^5)$	2	($\bar{1}$)	39	339
		4	($\bar{1}, \bar{1}$)	7	25
orthorhombic	$C2/c (C_{2h}^6)$	4	(1)	5	13
	$Cmca (D_{2h}^{18})$	4	(2/m)	1	3

^a The class is identified by space group, number of Z molecules in the unit cell, and site symmetry. For each class, we indicate the number of distinct minima and the total number of minima including duplicates.

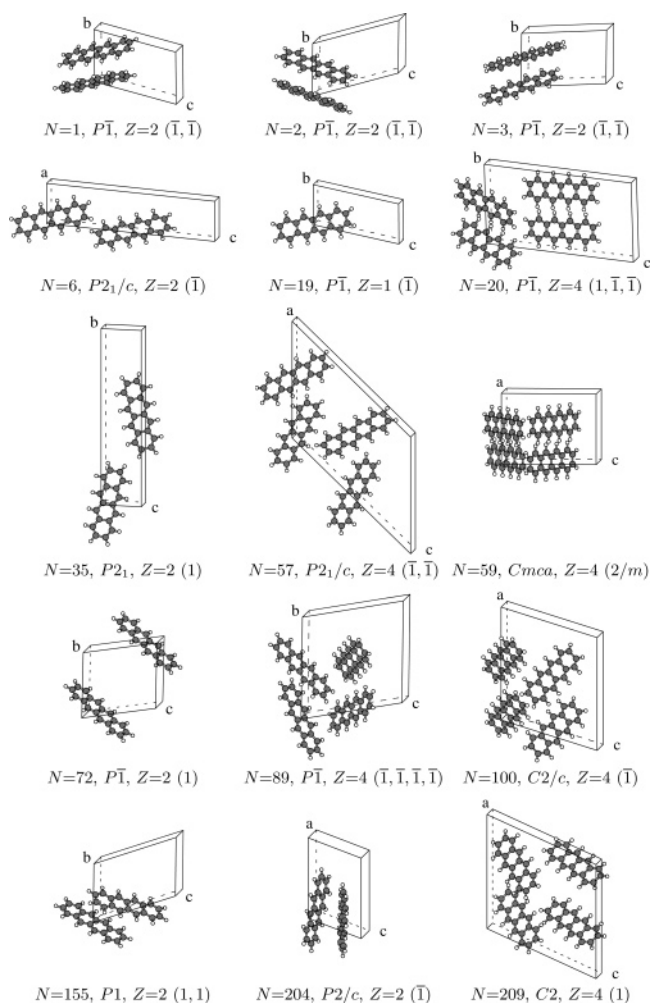


Figure 1. Structure of selected minima, shown with an orientation in which the shortest cell axis (either a or b) is approximately perpendicular to the plane of the page. Minima are labeled by their energy rank N (also indicated in Table 2) and structural class (space group, Z , and site symmetry).

structures we report in Table 2 the molar potential energy, density, structural class, crystallographic parameters, and a measure of accessibility, represented by the number of times M the minimum has been encountered.

It is remarkable that the three deepest minima, all in the same structural class, exhibit the layered herringbone packing char-

TABLE 2: Data for Selected Minima^a

<i>N</i>	energy	density	space group	<i>Z</i>	site symmetry	<i>a</i>	<i>b</i>	<i>c</i>	α	β	γ	<i>M</i>
1	-36.262	1.3886	$P\bar{1}$ (C_i^1)	2	$(\bar{1}, \bar{1})$	5.814	7.708	12.601	101.34	98.27	93.54	56
2	-35.909	1.3803	$P\bar{1}$ (C_i^1)	2	$(\bar{1}, \bar{1})$	5.941	7.588	12.806	73.88	82.02	85.59	18
3	-35.637	1.3767	$P\bar{1}$ (C_i^1)	2	$(\bar{1}, \bar{1})$	5.913	7.694	12.219	86.85	83.40	85.95	41
6	-32.902	1.3859	$P2_1/c$ (C_{2h}^5)	2	$(\bar{1})$	5.845	3.823	24.530	90.00	94.34	90.00	5
19	-31.970	1.3648	$P\bar{1}$ (C_i^1)	1	$(\bar{1})$	3.737	5.886	12.873	99.65	95.31	92.15	68
20	-31.912	1.3421	$P\bar{1}$ (C_i^1)	4	$(1, \bar{1}, \bar{1})$	4.431	12.013	21.572	94.94	91.47	99.03	1
35	-31.134	1.3417	$P2_1$ (C_2^2)	2	$(\bar{1})$	3.700	25.685	5.964	90.00	95.05	90.00	1
57	-30.576	1.3226	$P2_1/c$ (C_{2h}^5)	4	$(\bar{1}, \bar{1})$	16.993	3.911	23.739	90.00	133.45	90.00	2
59	-30.526	1.2780	$Cmca$ (D_{2h}^{18})	4	$(2/m)$	10.161	8.553	13.640	90.00	90.00	90.00	3
72	-30.177	1.3264	$P\bar{1}$ (C_i^1)	2	$(\bar{1})$	6.015	9.389	10.698	81.50	73.81	82.33	1
89	-29.835	1.2916	$P\bar{1}$ (C_i^1)	4	$(\bar{1}, \bar{1}, \bar{1})$	5.549	14.673	14.731	79.53	85.23	85.64	1
100	-29.560	1.3136	$C2/c$ (C_{2h}^6)	4	$(\bar{1})$	16.443	5.020	14.536	90.00	106.01	90.00	5
155	-28.589	1.2835	$P1$ (C_1^1)	2	$(1, \bar{1})$	5.969	8.460	12.443	71.04	83.52	86.18	2
204	-27.702	1.2474	$P2/c$ (C_{2h}^4)	2	$(\bar{1})$	11.705	6.737	8.168	90.00	109.47	90.00	1
209	-27.662	1.2507	$C2$ (C_2^3)	4	(1)	16.623	4.592	17.269	90.00	113.22	90.00	1

^a For each minimum, after the rank *N*, we report the molar potential energy (kcal/mol), density (g/cm³), structural class (space group, *Z*, and site symmetry), lattice parameters (axes *a*, *b*, and *c* in Å, and angles α , β , and γ in degrees), and number of times *M* it has been encountered. We list the three deepest minima (*N* = 1–3), combined with the lowest minimum in each structural class (*N* = 1, 6, and above).

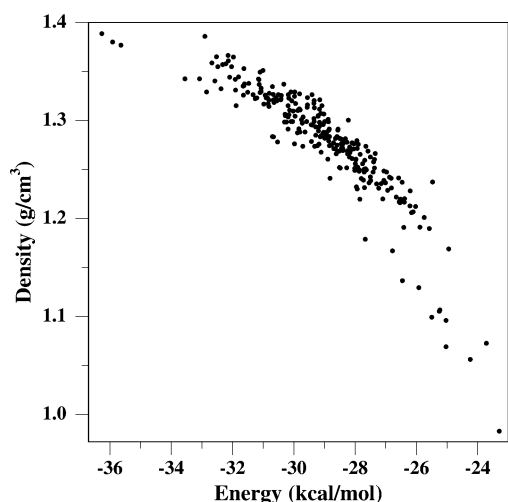


Figure 2. Density of the minima as a function of their energy.

acteristic of all known crystalline phases of tetracene and pentacene.^{6–10} There are always two translationally inequivalent molecules per unit cell (*Z* = 2), sitting on layers parallel to the *ab*-plane (with *a* and *b* being the two shorter cell axes). The long molecular axis is approximately perpendicular to the plane of the layer, and neighboring molecules within a layer are twisted with respect to each other, forming a herringbone pattern. This arrangement, which may evidently lead to stable and dense structures, is encountered quite frequently among the sampled minima.

As shown in Figure 1 and as already noticed for pentacene,¹⁶ deep minima exhibit a tendency toward closely packed arrangements in which the longitudinal axes of different molecules remain approximately aligned, whereas shallow minima present less efficient arrangements with looser structures. This finding, together with the observation that in Table 2 the deepest and most accessible minima also present high density, confirms that the packing efficiency has a significant effect on the energy.¹⁶ Like for pentacene, and as illustrated in Figure 2, we find a strong correlation between the energy and the density of the minima.

The distribution of the deepest minima appearing in Figure 2, however, is quite different from that for pentacene. For tetracene, in fact, we find only three minima near the potential bottom. As shown by Table 2, these three minima (energy rank *N* = 1, 2, 3) are all within 0.65 kcal/mol of the bottom. The next minimum (*N* = 4) is found at 2.70 kcal/mol above the

bottom, after a sizable energy gap. For pentacene,¹⁶ instead, we encountered a continuous distribution of energies, with a significant congestion of competing minima near the bottom. The deep minima for crystalline tetracene also seems to be less varied than for pentacene. The three deepest minima just mentioned, like the next two, all present triclinic unit cells, space group $P\bar{1}$, with two independent molecules on inversion sites, *Z* = 2 ($\bar{1}, \bar{1}$). This is by far the most frequent structural class. As shown in Table 2, the first minimum in a different class is a high-density monoclinic structure at rank *N* = 6, about 3.35 kcal/mol above the bottom. For pentacene, instead, we had already encountered four different structural classes in the range up to *N* = 6, in a much narrower energy interval (≈ 1.2 kcal/mol).

Presence of a gap, larger energy spread, and reduced variety of structures all indicate that the mathematical problem of finding the global minimum is somewhat easier for tetracene than for pentacene. There might be some physical reality behind this mathematical difference, since pentacene has a surprisingly large number of distinct polymorphs,^{4–6} whereas this does not seem to be the case for tetracene.

3.2. Comparison with the Experimental Structures. Once we found the potential minima,²¹ we compared them to the known experimental structures.^{8–11} We recall that for pentacene the two deepest minima were found to correspond to the two distinct polymorphs with completely described X-ray structures.¹⁶ For tetracene the most common form, namely polymorph I, certainly corresponds to the deepest minimum (labeled by *N* = 1 in Figure 1 and Table 2). In fact, this minimum is identical to that reached by starting from each one of the three complete X-ray structures.^{8–10} Since the measurements are at nonzero temperature, the comparison between computed and experimental structures is more accurate if one accounts for the effects of temperature, as we have done in the previous work²¹ by using quasi harmonic lattice dynamics (QHLD) methods^{38–40} to evaluate the Gibbs energy $G(p, T)$ as a function of pressure *p* and temperature *T*. We discovered that the structure of the deepest minimum, recomputed by accounting for the appropriate temperatures, reproduced quite well the measurements^{8,9} both at room conditions and at 183 K. The experimental sublimation heat⁴¹ was also well reproduced.²¹

It is very tempting to identify the second minimum (*N* = 2) with polymorph II. Unfortunately, a reliable comparison between the computed structures of the minima and the measurements for polymorph II is not feasible, since only the cell parameters

were experimentally determined,¹¹ while the space group and the atomic coordinates are unknown. Even the comparison with the published cell axes and angles is not very reliable, since the cell parameters can be chosen in many different ways and are very sensitive to small changes in the angles closer to 90°, especially for triclinic systems. In the previous paper²¹ we could find a choice for the cell of the second minimum, recomputed by accounting for the temperature, which compared favorably with the experimental cell parameters of polymorph II at 140 K.¹¹ It should also be stressed that the assignment of polymorphs I and II to the two deepest minima is supported²¹ by the good match between the frequencies of the lattice phonons computed for the two minima and the experimental Raman spectra of the two polymorphs. The spectra computed for the next few minima are remarkably different. These comparisons are less ambiguous than the comparison between the lattice parameters, since they are independent of the cell choice. As discussed in the Introduction, this strategy was very successful for pentacene, for which the assignments initially obtained only by matching experimental and calculated spectra¹⁷ were finally confirmed by the X-ray diffraction measurements.¹⁹

4. Discussion and Conclusions

We have presented the results of a systematic sampling of the potential energy surface of crystalline tetracene, performed to identify the possible polymorphs of this compound. Hundreds of distinct minima have been encountered, with a large variety of structural arrangements. The deepest minimum corresponds to the known high temperature–low pressure form (polymorph I),^{8–10} while the next deepest minimum most probably corresponds to the low temperature–high pressure form (polymorph II), identified by X-ray¹¹ and Raman²¹ experiments, but whose structure has not yet been fully described. It may be noticed that the only previously published prediction of the crystal structures of tetracene and pentacene⁴² could not possibly succeed in locating these deep minima, because the search was restricted to crystals with a single independent molecule in the unit cell.

The majority of minima (≈63%), including all easily accessible deep minima up to rank $N = 5$, present triclinic structures with space group $P\bar{1}$ (C_i^1) and two molecules per unit cell, both residing on symmetry unrelated inversion centers. For this reason, it is a safe bet that the most easily obtained polymorphs will also belong to this very common^{35–37} structural class, namely $P\bar{1}$ with $Z = 2$ ($\bar{1}$, $\bar{1}$). For polymorph I this is a known experimental fact,^{8–10} while for polymorph II this is the only reasonable possibility consistent with both X-ray¹¹ and Raman²¹ experiments. With comparable confidence, we can also assert that polymorph II has a layered herringbone structure similar to that of polymorph I. For most practical purposes, it may be thus concluded that the precise rank of the minima does not really matter much.

In any case, it must be stressed that we have ranked the possible structures by their lattice energy, computed with a specific potential model. The possibilities and limitations of this strategy, in which the potential energy is the only selection criterion, have been assessed by the recent blind tests of crystal structure prediction.^{43–45} Since entropic and kinetic factors certainly play a role during crystallization, additional ranking criteria, besides the potential energy, have been considered in the tests. The vibrational contribution to the Gibbs energy has been taken into account, and there have been attempts to relate kinetic effects to other calculated quantities (such as structural isotropy and mechanical or morphological properties). At least

for the molecules in the blind tests, these attempts did not lead to improved reordering of the possible structures.⁴⁵ This also holds for tetracene, for which we have found that adding the vibrational contribution to the Gibbs energy, computed as mentioned in the previous section, does not alter the rank of the deepest minima. We have also partially investigated the role of the potential model, by removing the Coulombic interactions from the model. Again, we found no rank changes for the deep minima.

The disappointing overall performance of the blind tests^{43–45} clearly indicates that a generally satisfactory prediction strategy is not yet available. Furthermore, as indicated by a survey of nearly 200 prediction studies,⁴⁶ while many structures may be readily predicted, it remains very difficult to judge which molecular types should be expected to lead to successful predictions. For this reason the excellent results for pentacene¹⁶ and tetracene,²¹ which suggest that successful predictions are attainable for the acenes, appear particularly significant.

Acknowledgment. Work done with funds from MIUR (PRIN 2003 and FIRB-RBNE01P4JF through INSTM consortium).

References and Notes

- (1) de Boer, R. W. I.; Jochemsen, M.; Klapwijk, T. M.; Morpurgo, A. F.; Niemax, J.; Tripathi, A. K.; Pflaum, J. *J. Appl. Phys.* **2004**, *95*, 1196.
- (2) Rang, Z.; Nathan, M. I.; Ruden, P. P.; Chesterfield, R.; Frisbie, C. D. *Appl. Phys. Lett.* **2004**, *85*, 5760.
- (3) Goldmann, C.; Haas, S.; Krellner, C.; Pernstich, K. P.; Gundlach, D. J.; Batlogg, B. *J. Appl. Phys.* **2004**, *96*, 2080.
- (4) Bouchoms, I. P. M.; Schoonveld, W. A.; Vrijmoeth, J.; Klapwijk, T. M. *Synth. Met.* **1999**, *104*, 175.
- (5) Gundlach, D. J.; Jackson, T. N.; Schlom, D. G.; Nelson, S. F. *Appl. Phys. Lett.* **1999**, *74*, 3302.
- (6) Mattheus, C. C.; Dros, A. B.; Baas, J.; Meetsma, A.; de Boer, J. L.; Palstra, T. T. M. *Acta Crystallogr., Sect. C: Cryst. Struct. Commun.* **2001**, *57*, 939.
- (7) Siegrist, T.; Kloc, Ch.; Schön, J. H.; Batlogg, B.; Haddon, R. C.; Berg, S.; Thomas, G. A. *Angew. Chem., Int. Ed. Engl.* **2001**, *40*, 1732.
- (8) Holmes, D.; Kumaraswamy, S.; Matzger, A. J.; Vollhardt, K. P. *Chem. Eur. J.* **1999**, *5*, 3399.
- (9) Campbell, R. B.; Robertson, J. M.; Trotter, J. *Acta Crystallogr.* **1962**, *15*, 289.
- (10) Robertson, J. M.; Sinclair, V. C.; Trotter, J. *Acta Crystallogr.* **1961**, *14*, 697.
- (11) Sondermann, U.; Kutoglu, A.; Bässler, H. *J. Phys. Chem.* **1985**, *89*, 1735.
- (12) Rang, Z.; Haraldsson, A.; Kim, D. M.; Ruden, P. P.; Nathan, M. I.; Chesterfield, R. J.; Frisbie, C. D. *Appl. Phys. Lett.* **2001**, *79*, 2731.
- (13) de Boer, R. W. I.; Klapwijk, T. M.; Morpurgo, A. F. *Appl. Phys. Lett.* **2003**, *83*, 4345.
- (14) Venuti, E.; Della Valle, R. G.; Brillante, A.; Masino, M.; Girlando, A. *J. Am. Chem. Soc.* **2002**, *124*, 2128.
- (15) Masino, M.; Girlando, A.; Della Valle, R. G.; Venuti, E.; Farina, L.; Brillante, A. *Mater. Res. Soc. Symp. Proc.* **2002**, *725*, P10.4.1.
- (16) Della Valle, R. G.; Venuti, E.; Brillante, A.; Girlando, A. *J. Chem. Phys.* **2003**, *118*, 807.
- (17) Brillante, A.; Della Valle, R. G.; Farina, L.; Girlando, A.; Masino, M.; Venuti, E. *Chem. Phys. Lett.* **2002**, *357*, 32.
- (18) Della Valle, R. G.; Venuti, E.; Farina, L.; Brillante, A.; Girlando, A.; Masino, M. *Org. Electron.* **2004**, *5*, 1.
- (19) Farina, L.; Brillante, A.; Della Valle, R. G.; Venuti, E.; Amboage, M.; Syassen, K. *Chem. Phys. Lett.* **2003**, *375*, 490.
- (20) Stillinger, F. H.; Weber, T. A. *Phys. Rev. A* **1982**, *25*, 978.
- (21) Venuti, E.; Della Valle, R. G.; Farina, L.; Brillante, A.; Masino, M.; Girlando, A. *Phys. Rev. B* **2004**, *70*, 104106.
- (22) Jankowiak, R.; Kalinowski, J.; Konys, M.; Buchert, J. *Chem. Phys. Lett.* **1979**, *65*, 549.
- (23) Kalinowski, J.; Jankowiak, R. *Chem. Phys. Lett.* **1978**, *53*, 56.
- (24) Press, W. H.; Teukolsky, S. A.; Vetterling, W. T.; Flannery, B. P. *Numerical Recipes in Fortran*; Cambridge University Press: Cambridge, 1992.
- (25) Lee, C.; Yang, W.; Parr, R. G. *Phys. Rev. B* **1988**, *37*, 785.
- (26) Pertsin, A. J.; Kitaigorodsky, A. I. *The Atom-Atom Potential Method*; Springer-Verlag: Berlin, 1987.
- (27) Williams, D. E. *J. Chem. Phys.* **1967**, *47*, 4680.

- (28) Frisch, M. J.; Trucks, G. W.; Schlegel, H. B.; Scuseria, G. E.; Robb, M. A.; Cheeseman, J. R.; Montgomery, J. A., Jr.; Vreven, T.; Kudin, K. N.; Burant, J. C.; Millam, J. M.; Iyengar, S. S.; Tomasi, J.; Barone, V.; Mennucci, B.; Cossi, M.; Scalmani, G.; Rega, N.; Petersson, G. A.; Nakatsuji, H.; Hada, M.; Ehara, M.; Toyota, K.; Fukuda, R.; Hasegawa, J.; Ishida, M.; Nakajima, T.; Honda, Y.; Kitao, O.; Nakai, H.; Klene, M.; Li, X.; Knox, J. E.; Hratchian, H. P.; Cross, J. B.; Bakken, V.; Adamo, C.; Jaramillo, J.; Gomperts, R.; Stratmann, R. E.; Yazyev, O.; Austin, A. J.; Cammi, R.; Pomelli, C.; Ochterski, J. W.; Ayala, P. Y.; Morokuma, K.; Voth, G. A.; Salvador, P.; Dannenberg, J. J.; Zakrzewski, V. G.; Dapprich, S.; Daniels, A. D.; Strain, M. C.; Farkas, O.; Malick, D. K.; Rabuck, A. D.; Raghavachari, K.; Foresman, J. B.; Ortiz, J. V.; Cui, Q.; Baboul, A. G.; Clifford, S.; Cioslowski, J.; Stefanov, B. B.; Liu, G.; Liashenko, A.; Piskorz, P.; Komaromi, I.; Martin, R. L.; Fox, D. J.; Keith, T.; Al-Laham, M. A.; Peng, C. Y.; Nanayakkara, A.; Challacombe, M.; Gill, P. M. W.; Johnson, B.; Chen, W.; Wong, M. W.; Gonzalez, C.; Pople, J. A. *Gaussian 98, Revision A.7*; Gaussian Inc.: Pittsburgh, PA, 1998.
- (29) Le Page, Y. *J. Appl. Crystallogr.* **1987**, *20*, 264. Le Page, Y. *J. Appl. Crystallogr.* **1988**, *21*, 983.
- (30) Schmidt, M. U.; Englert, U. *J. Chem. Soc., Dalton. Trans.* **1996**, 2077.
- (31) Busing, W. R.; Matsui, M. *Acta Crystallogr., Sect. A: Found. Crystallogr.* **1984**, *40*, 532.
- (32) Signorini, G. F.; Righini, R.; Schettino, V. *Chem. Phys.* **1991**, *154*, 245.
- (33) Spek, A. L. *J. Appl. Crystallogr.* **2003**, *36*, 7. <http://www.cryst.chem.uu.nl/platon/>.
- (34) Kraulis, P. J. *J. Appl. Crystallogr.* **1991**, *24*, 946. <http://www.avatar.se/molscript/>.
- (35) Belsky, V. K.; Zorkii, P. M. *Acta Crystallogr., Sect. A: Found. Crystallogr.* **1977**, *33*, 1004.
- (36) Belsky, V. K.; Zorkaya, O. N.; Zorkii, P. M. *Acta Crystallogr., Sect. A: Found. Crystallogr.* **1995**, *51*, 473.
- (37) Mighell, A. D.; Rodgers, J. R. *Acta Crystallogr., Sect. A: Found. Crystallogr.* **1980**, *36*, 321.
- (38) Ludwig, W. *Recent Developments in Lattice Theory*; Springer-Verlag: Berlin, 1967; Springer Tracts in Modern Physics, Vol. 43.
- (39) Della Valle, R. G.; Venuti, E.; Brillante, A. *Chem. Phys.* **1996**, *202*, 231.
- (40) Della Valle, R. G.; Venuti, E. *Phys. Rev. B* **1998**, *58*, 206.
- (41) DeKruif, C. G. *J. Chem. Thermodyn.* **1980**, *12*, 243.
- (42) Chaka, A. M.; Zaniewski, R.; Youngs, W.; Tessier, C.; Klopman, G. *Acta Crystallogr., Sect. B: Struct. Sci.* **1996**, *52*, 165.
- (43) Lommerse, J. P. M. *Acta Crystallogr., Sect. B: Struct. Sci.* **2000**, *56*, 697.
- (44) Motherwell, W. D. S. *Acta Crystallogr., Sect. B: Struct. Sci.* **2002**, *58*, 647.
- (45) Day, G. M.; Motherwell, W. D. S.; Ammon, H. L.; Boerrigter, S. X. M.; Della Valle, R. G.; Venuti, E.; Dzyabchenko, A.; Dunitz, J. D.; Schweizer, B.; van Eijck, B. P.; Erk, P.; Facelli, J. C.; Bazterra, V. E.; Ferraro, M. B.; Hofmann, D. W. M.; Leusen, F. J. J.; Liang, C.; Pantelides, C. C.; Karamertzanis, P. G.; Price, S. L.; Lewis, T. C.; Nowell, H.; Torrisi, A.; Scheraga, H. A.; Arnautova, Y. A.; Schmidt, M. U.; Verwer, P. *Acta Crystallogr., Sect. B: Struct. Sci.* **2005**, *61*, 511.
- (46) Beyer, T.; Lewis, T.; Price, S. L. *CrystEngComm* **2001**, *44*, 1.